

Supporting Information

# **Influences of Side Chain and Substrate on Polythiophene Thin Film Surface, Bulk, and Buried Interfacial Structures**

*Minyu Xiao<sup>1</sup>, Joshua Jasensky<sup>1</sup>, Xiaoxian Zhang<sup>2</sup>, Yaxin Li<sup>1</sup>, Cayla Pichan<sup>1</sup>, Xiaolin Lu<sup>3</sup>,  
Zhan Chen<sup>1\*</sup>*

*<sup>1</sup>Department of Chemistry, University of Michigan, Ann Arbor, Michigan, 48109-1055, USA*

*<sup>2</sup>Key laboratory of Standardization and Measurement for Nanotechnology, Chinese Academy  
of Sciences, National Center for Nanoscience and Technology, Beijing 100190, China*

*<sup>3</sup>State Key Laboratory of Bioelectronics, School of Biological Science and Medical  
Engineering, Southeast University, Nanjing 210096, China.*

*\*Corresponding author: Zhan Chen (zhanc@umich.edu)*

## 1. SFG Introduction:

SFG theory, data interpretation, and surface selectivity have been extensively published previously.<sup>1-11</sup> Briefly, SFG output intensity can be expressed as:

$$I_{SFG} \propto |\chi_{eff}^{(2)}|^2 I_{IR} I_{vis} \quad (1)$$

where the  $I_{IR}$  and  $I_{vis}$  are the input IR and visible beam intensities.  $\chi_{eff}^{(2)}$  is the effective second-order nonlinear optical susceptibility of the surface/interface, expressed as:

$$\chi_{eff}^{(2)} = \chi_{NR}^{(2)} + \sum_q \frac{A_q}{\omega_{IR} - \omega_q + i\Gamma_q} \quad (2)$$

$\chi_{NR}^{(2)}$  is the nonresonant contribution from the sample. The resonant part of equation 2 can be fitted as a sum of Lorentzian peaks with a peak strength of  $A_q$ , frequency of  $\omega_q$ , and a peak width of  $\Gamma_q$  for the peak q. All the SFG spectra in this paper are fitted with equation 2.  $\chi_{eff}^{(2)}$  is the effective second-order nonlinear susceptibility tensor of the sample (e.g., a surface or an interface), which is correlated to the second-order nonlinear susceptibility tensor  $\chi^{(2)}$  defined in the lab fixed coordinate system. Therefore, different tensor components of  $\chi^{(2)}$  can be deduced from different components of  $\chi_{eff}^{(2)}$ . To do so, it is necessary to measure different components of  $\chi_{eff}^{(2)}$  using different output/input beam polarization combinations in the SFG experiment.

SFG signal collected from a thin film on a substrate may originate from both the surface and the buried film/substrate interface. Such a signal is dependent on the thickness of the film.<sup>12,13</sup> Detailed data analysis methods on SFG spectra collected from a thin film with various models have been reported elsewhere.<sup>14-16</sup> Details of our SFG spectrometers and SFG data collection have been published and will not be repeated here. In the current experiments, the incident angles of the input visible and IR beams are 60° and 55° versus the surface normal, as reported previously.

## 2. Refractive indices:

	Visible region	IR region
Silicon	4.2	3.8
P3HT	2.2	1.8
Air	1.0	1.0
Gold	0.54+2.14i	6.28+42.9i

Tab S1 Refractive indices of all the materials used for Fresnel coefficient calculation<sup>17-19</sup>

## 3. SFG spectra from P3HT film on Si before and after short time plasma treatment:

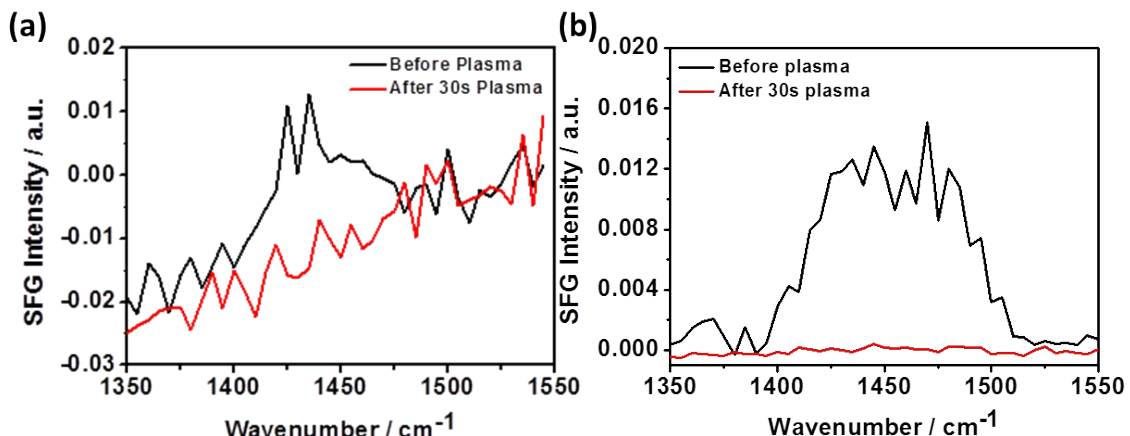


Fig S1 (a) SFG SSP spectra collected from a P3HT film on a silicon substrate before and after 30 s air plasma treatment; (b) SFG PPP spectra collected from a P3HT film on a silicon substrate before and after 30s air plasma treatment.

Fig S1 shows that both SFG SSP and PPP spectra detected from a P3HT film deposited on Si vanished after 30 s air plasma treatment on the P3HT film surface. Since a short time air plasma treatment can only destroy the surface structure, not the buried interfacial structure, the above observation confirms that the SFG signal was contributed from the surface of the P3HT film on silicon wafer.

## 4. Calculating the dependence of $|\chi_{\text{eff},\text{PPP}}^{(2)} / \chi_{\text{eff},\text{SSP}}^{(2)}|$ on the tilt angle ( $C_{2v}$ symmetry), and spectral fitting details:

For  $C_{2v}$  symmetry:

$$\chi_{XXZ} = \chi_{YYZ} = \frac{1}{2} N_s \times \begin{cases} \langle \sin^2 \theta \cos \theta \rangle (\beta_{zzz}) + \langle \cos \theta \rangle (\beta_{xxz} + \beta_{yyz}) \\ - \langle \sin^2 \theta \cos \theta \sin^2 \psi \rangle (\beta_{yyz} + \beta_{zyx} + \beta_{zyy}) \\ - \langle \sin^2 \theta \cos \theta \sin^2 \psi \rangle (\beta_{xxz} + \beta_{xzx} + \beta_{zxx}) \end{cases} \quad (\text{eq S1})$$

$$\chi_{YXZ} = \frac{1}{2} N_s \times \begin{cases} \langle \sin^2 \theta \cos \theta \rangle (\beta_{zzz}) + \langle \cos \theta \rangle (\beta_{xxx} + \beta_{yyz}) \\ -\langle \sin^2 \theta \cos \theta \sin^2 \psi \rangle (\beta_{yyz} + \beta_{yzy} + \beta_{zyy}) \\ -\langle \sin^2 \theta \cos \theta \sin^2 \psi \rangle (\beta_{xxz} + \beta_{xzx} + \beta_{zxx}) \end{cases} \quad (\text{eq S2})$$

$$\chi_{ZXZ} = \frac{1}{2} N_s \times \begin{cases} \langle \sin^2 \theta \cos \theta \rangle (\beta_{zzz}) + \langle \cos \theta \rangle (\beta_{zxx} + \beta_{zyy}) \\ -\langle \sin^2 \theta \cos \theta \sin^2 \psi \rangle (\beta_{yyz} + \beta_{yzy} + \beta_{zyy}) \\ -\langle \sin^2 \theta \cos \theta \sin^2 \psi \rangle (\beta_{xxz} + \beta_{xzx} + \beta_{zxx}) \end{cases} \quad (\text{eq S3})$$

$$\chi_{ZZZ} = N_s \times \begin{cases} \langle \cos^3 \theta \rangle (\beta_{zzz}) \\ +\langle \sin^2 \theta \cos \theta \sin^2 \psi \rangle (\beta_{yyz} + \beta_{yzy} + \beta_{zyy}) \\ +\langle \sin^2 \theta \cos \theta \cos^2 \psi \rangle (\beta_{xxz} + \beta_{xzx} + \beta_{zxx}) \end{cases} \quad (\text{eq S4})$$

Deduced from eq S1, eq S2, eq S3, eq S4,  $|\chi_{\text{eff},\text{PPP}}^{(2)} / \chi_{\text{eff},\text{SSP}}^{(2)}|$  obtained from different polarization combination can be expressed as:

$$|\chi_{\text{eff},\text{PPP}}^{(2)} / \chi_{\text{eff},\text{SSP}}^{(2)}| = \frac{\begin{vmatrix} -L_{xx}(\omega) L_{xx}(\omega_1) L_{zz}(\omega_2) \cos \beta \cos \beta_1 \sin \beta_2 \chi_{xxz} \\ -L_{xx}(\omega) L_{zz}(\omega_1) L_{xx}(\omega_2) \cos \beta \sin \beta_1 \cos \beta_2 \chi_{zxx} \\ +L_{zz}(\omega) L_{xx}(\omega_1) L_{xx}(\omega_2) \sin \beta \cos \beta_1 \cos \beta_2 \chi_{xxx} \\ +L_{zz}(\omega) L_{zz}(\omega_1) L_{zz}(\omega_2) \sin \beta \sin \beta_1 \sin \beta_2 \chi_{xxz} \end{vmatrix}}{|L_{yy}(\omega) L_{yy}(\omega_1) L_{zz}(\omega_2) \sin \beta_2 \chi_{yyz}|} \quad (\text{eq S5})$$

Detailed Fresnel coefficient values can be obtained from Fig 3 in the main context, and hyperpolarizability tensor component values have been published elsewhere.<sup>20,21</sup> Briefly,

$$\frac{\beta_{aac}}{\beta_{ccc}} \approx 70 \text{ and } \frac{\beta_{bbc}}{\beta_{ccc}} \approx -1.$$

Therefore, the  $|\chi_{\text{eff},\text{PPP}}^{(2)} / \chi_{\text{eff},\text{SSP}}^{(2)}|$  ratio depends on the tilt angle and the twist angle  $(\theta, \psi)$ . When a uniform distribution of twist angle  $\psi$  is assumed, values of  $\sin(\psi)$  and  $\cos(\psi)$  can be obtained based on the assumed twist angle  $\psi$ .

Fitting parameters of the SFG spectra presented in Fig 5 and Fig 6 are listed in Tab S2 below:

-CH3 (PPP/SSP) 1.73		-CF3 (PPP/SSP) 1.63		PDMS (PPP/SSP) 1.72	
A	17.1/9.9	A	17.8/9.7	A	8.6/5.0
x	1445/1445	x	1445/1445	x	1445/1445
W	22.7/22.7	W	27.0/23.9	W	22.0/22.0
-C6H5 (PPP/SSP) 1.35		-NH2 (PPP/SSP) 1.19		PVA (PPP/SSP) 1.19	
A	17.8/13.2	A	16.2/13.6	A	5.7/4.8
x	1445/1445	x	1445/1445	x	1445/1445
W	25.6/25.6	W	22.6/22.6	W	23.9/23.8
Si (PPP/SSP) 0.95		P3KHT 50%CH3 50%NH2 1.98		P3KHT -C6H5 1.52	
A	17.7/17	A	16.8/8.2	A	17.3/11.4
x	1445/1445	x	1440/1440	x	1440/1440
W	23.2/23.5	W	20.2/19.9	W	20.0/20.0
P3KHT -NH2 1.36		P3KHT Si 1.09			
A	17.9/12.8	A	14.7/13.8		

x	1440/1440	x	1440/1440	
W	19.2/20.1	W	20.4/20.5	

Tab S2 Fitting parameters of SFG spectra from Fig 5 and Fig 6.

### 5. UV-Vis of P3HT, P3KHT thin films on various different surfaces:

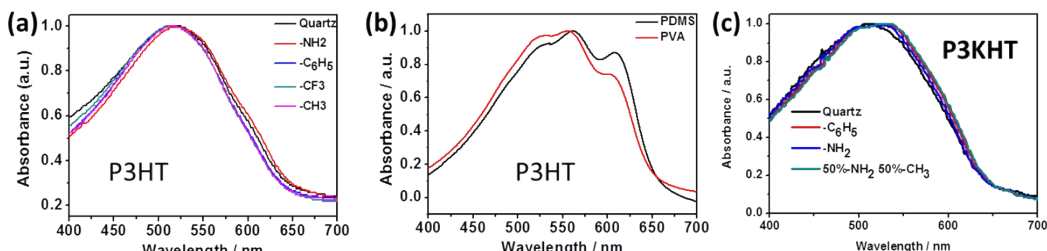


Fig S2 P3HT and P3KHT thin film UV-Vis on various different surfaces.

### 6. XPS characterization of SAM surfaces:

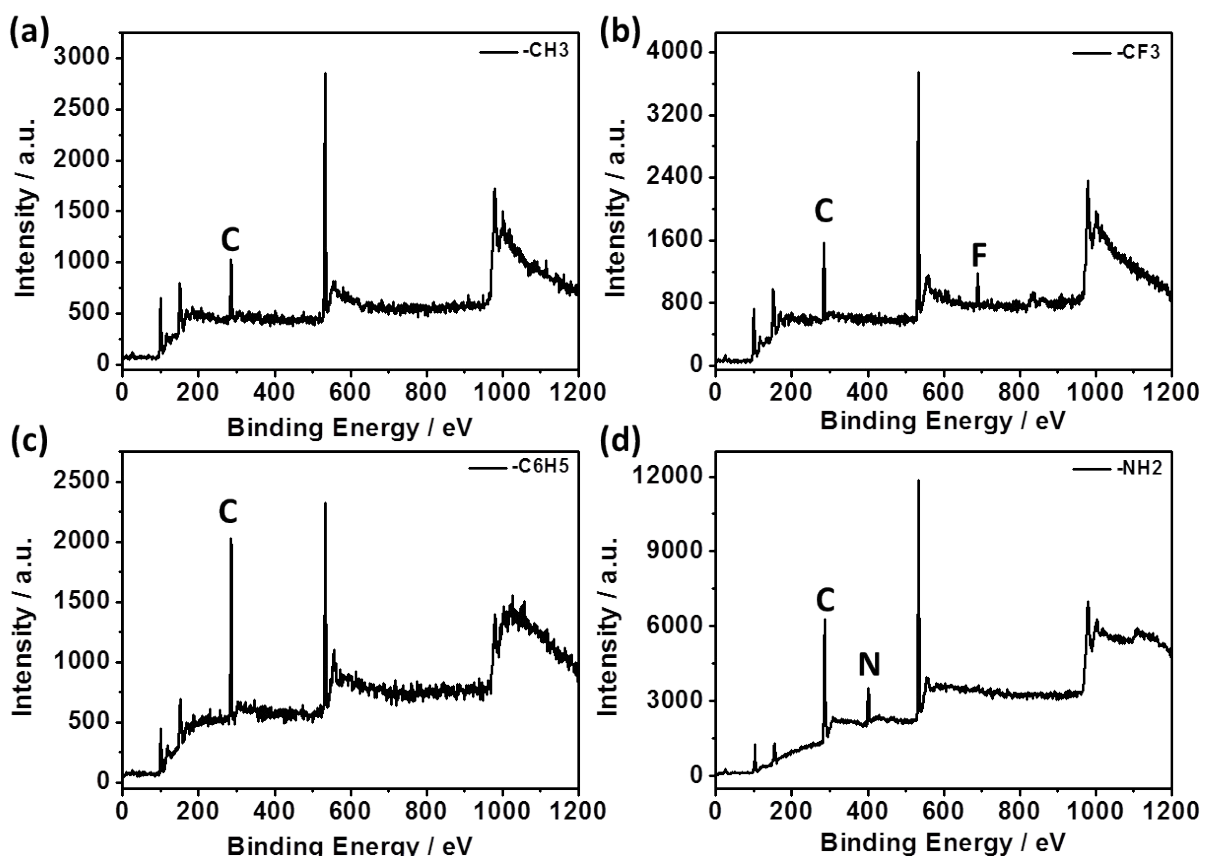


Fig S3 XPS signals detected from the following SAM surfaces: (a) methyl terminated SAM surface; (b) trifluoromethyl terminated SAM surface; (c) phenyl terminated SAM surface; (d) amine terminated SAM surface;

Figure S3 shows the XPS signals collected from different SAM surfaces. Both methyl and phenyl group terminated SAM surfaces show a strong C1s peak at ~300eV; the trifluoromethyl terminated SAM surface shows a F1s peak at ~680eV in addition to the C1s

signal; the amine terminated SAM surface shows a N1s peak at ~400eV in addition to the C1s signal.<sup>22-24</sup>

## 7. SFG signal origin and plasma treatment effect in P3HT/Gold geometry:

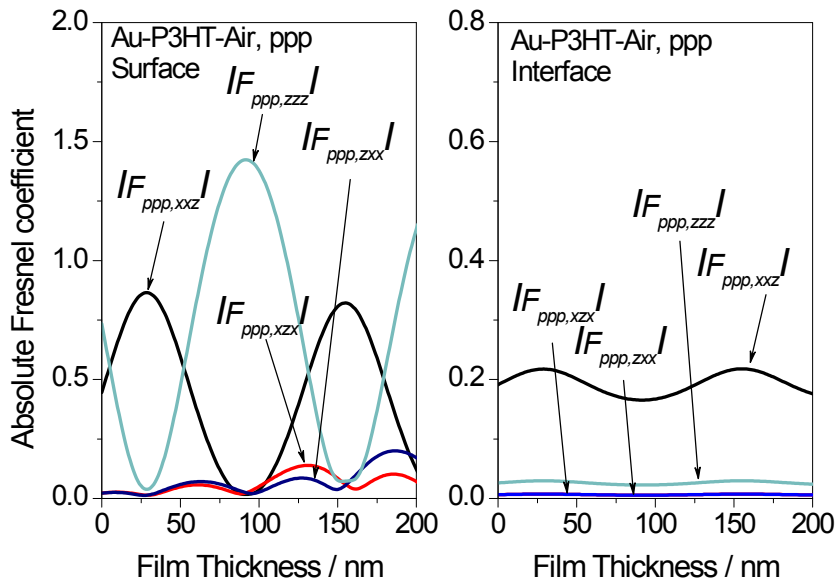


Fig S4 Fresnel coefficient values of zzz, zxx, xzx, xxz susceptibility tensor elements as a function of P3HT film thickness at the P3HT/air and P3HT/gold interfaces.

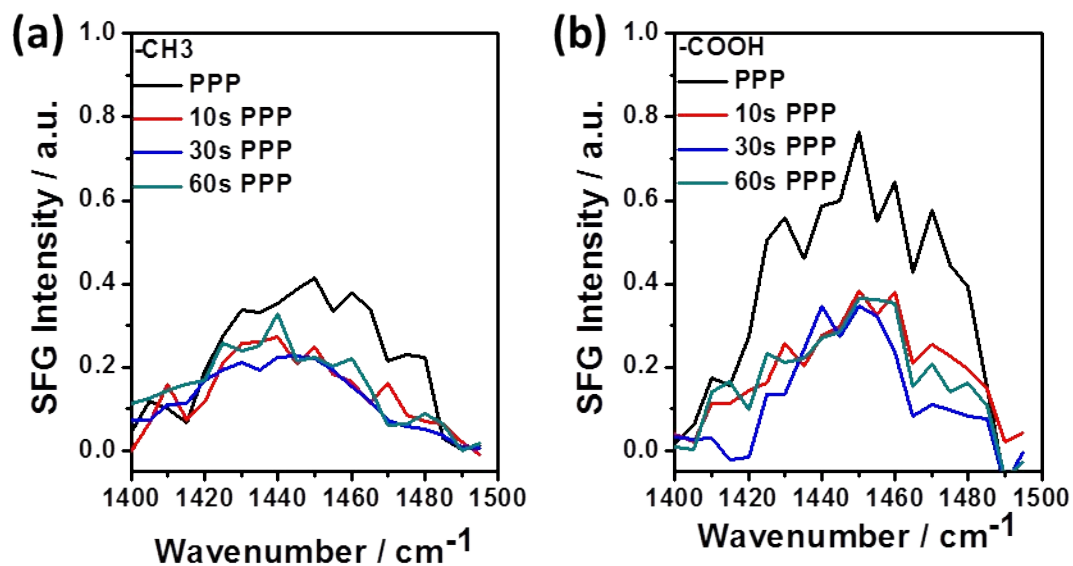


Fig S5 SFG PPP spectra collected from PsHT films: (a) Before and after brief plasma treatment of P3HT film on  $-\text{CH}_3$  terminated thiol surface; (b) Before and after brief plasma treatment of P3HT film on  $-\text{COOH}$  terminated thiol surface.

Reference:

- (1) Shen, Y. R. *Nature* **1989**, 337, 519.
- (2) Wang, J.; Chen, C.; Buck, S. M.; Chen, Z. *The Journal of Physical Chemistry B* **2001**, 105, 12118.
- (3) Su, X.; Cremer, P. S.; Shen, Y. R.; Somorjai, G. A. *Physical review letters* **1996**, 77, 3858.
- (4) Su, X.; Cremer, P. S.; Shen, Y. R.; Somorjai, G. A. *Journal of the American Chemical Society* **1997**, 119, 3994.
- (5) Chen, Z.; Shen, Y. R.; Somorjai, G. A. *Annual review of physical chemistry* **2002**, 53, 437.
- (6) Kim, J.; Chou, K. C.; Somorjai, G. A. *The Journal of Physical Chemistry B* **2003**, 107, 1592.
- (7) Kim, J.; Cremer, P. S. *Journal of the American Chemical Society* **2000**, 122, 12371.
- (8) Cong, X.; Poyton, M. F.; Baxter, A. J.; Pullanchery, S.; Cremer, P. S. *Journal of the American Chemical Society* **2015**, 137, 7785.
- (9) Yan, E. C. Y.; Fu, L.; Wang, Z.; Liu, W. *Chemical reviews* **2014**, 114, 8471.
- (10) Perry, A.; Ahlbom, H.; Space, B.; Moore, P. B. *The Journal of chemical physics* **2003**, 118, 8411.
- (11) Perry, A.; Neupert, C.; Space, B.; Moore, P. B. *Chemical reviews* **2006**, 106, 1234.
- (12) Myers, J. N.; Zhang, X.; Bielefeld, J. D.; Lin, Q.; Chen, Z. *The Journal of Physical Chemistry B* **2015**.
- (13) Lu, X.; Shephard, N.; Han, J.; Xue, G.; Chen, Z. *Macromolecules* **2008**, 41, 8770.
- (14) Backus, E. H. G.; Garcia-Araez, N.; Bonn, M.; Bakker, H. J. *The Journal of Physical Chemistry C* **2012**, 116, 23351.
- (15) Tong, Y.; Zhao, Y.; Li, N.; Osawa, M.; Davies, P. B.; Ye, S. *The Journal of chemical physics* **2010**, 133, 034704.
- (16) Lu, X.; Clarke, M. L.; Li, D.; Wang, X.; Xue, G.; Chen, Z. *The Journal of Physical Chemistry C* **2011**, 115, 13759.
- (17) Icenogle, H. W.; Platt, B. C.; Wolfe, W. L. *Applied optics* **1976**, 15, 2348.
- (18) Lee, W. H.; Chuang, S. Y.; Chen, H. L.; Su, W. F.; Lin, C. H. *Thin Solid Films* **2010**, 518, 7450.
- (19) Liu, X.; Atwater, M.; Wang, J.; Huo, Q. *Colloids and Surfaces B: Biointerfaces* **2007**, 58, 3.
- (20) Anglin, T. C.; Speros, J. C.; Massari, A. M. *The Journal of Physical Chemistry C* **2011**, 115, 16027.
- (21) Dhar, P.; Khlyabich, P. P.; Burkhardt, B.; Roberts, S. T.; Malyk, S.; Thompson, B. C.; Benderskii, A. V. *The Journal of Physical Chemistry C* **2013**, 117, 15213.
- (22) Wasserman, S. R.; Whitesides, G. M.; Tidswell, I. M.; Ocko, B. M.; Pershan, P. S.; Axe, J. D. *Journal of the American Chemical Society* **1989**, 111, 5852.

- (23) Bourg, M.-C.; Badia, A.; Lennox, R. B. *The Journal of Physical Chemistry B* **2000**, *104*, 6562.
- (24) Nielsen, J. U.; Esplandiu, M. J.; Kolb, D. M. *Langmuir* **2001**, *17*, 3454.